Sohag Journal of Sciences
An International Journal

http://dx.doi.org/10.18576/sjs/040101

The Effect of Recombination Losses on the efficiency CIGS Thin-Film Solar Cell

Hussein Mohmed [1,*] *and Abdelhai Mohamed* [2,3]

[1]Physics department, Faculty of Science, Sohag University, 82524 Sohag, Egypt.
[2]Department of Physics, College of Sciences, King Saud University, 11451 Riyadh, KSA.
[3]Physics department, Faculty of Science, Al-Azhar University, Cairo, Nasr City.

Received: 11 Aug. 2018, Revised: 28 Nov. 2018, Accepted: 7 Dec. 2018.

Abstract: This work focuses on stying the effect of recombination losses on the efficiency of thin-film solar cell based on CIGS. The results have been carried out based on the width of the space-charge region, thickness of the absorber layer, lifetimes of charge carriers and recombination velocity at the front and back surfaces. The recombination losses in thin-film solar cells based on CIGS have been evaluated quantitatively. The determination of the recombination losses is carried out on the basis of the continuity equation taking into account the drift and diffusion components of the photocurrent. It is found that the thickness of the absorber layer has a significant effect on the values of short-circuit current density more than the effect of the width of the space-charge region. The front surface recombination losses increased with widening W while the back surface recombination losses can be neglected particularly at thick layer of the absorber. The minimum recombination losses of 3% have been achieved for dCIGS>2 µm and W=0.3 µm. At certain parameters of the used materials and with taking into account recombination losses, the efficiency of CIGS records a value about 25%.

Keywords: CIGS solar cell - recombination losses; short-circuit current density- efficiency.

1 Introduction

Cu(InGa)Se2 (CIGS) thin-film solar cells have attracted great attention of academic and industrial researchers due to their superior properties and great prospects for further development [1–3]. The highest effi-ciency for a CIGS-based solar cell 23.35%, was obtained in 2019 [4], which has demonstrated CIGS solar cell.

The conversion efficiency of the typical structure of substrate CIGS solar cell consists of ZnO:Al/CdS/CIGS/Mo/Glass can reach 22% [5] and in modules is in the range12-15 % [6]. On the other hand, the theoretical limit of these solar cells is high and can reach 28-30% [6].

Unfortunately, this kind of solar cell with a single junction has limited efficiency, as the solar cell absorbs only the photons with energy higher than, or equal to, the used material energy gap; while the remainder of the incident spectrum will be wasted, and even photons with energies greater than the energy gap will lose the energy difference due to thermalization losses. This limitation can be overcome by select appropriate parameters of the used materials. Present day, high performance thin film CIGS solar cells however use more sophisticated band gap profiles, almost always involving a grading of the band gap throughout the absorber layer, consequently a changing of most material properties across the cell [7]. For example, the effect of the absorber layer band-gap was studied by Belghachi and Limam [8]. In their simulation, they found that maximum efficiency of about 23% can be achieved with a band gap of around 1.48 eV and this efficiency can be increased up to 24.34 % corresponding to an optimised back graded absorber of 1.41 eV gap at the front and 1.54 eV gap at the rear contact.

there are the recombination losses that take place at the front and back surface of CIGS.

The present work aims to study the effect of the recombination losses on the performance of CIGS solar cell with structure ZnO:Al/CdS/CIGS/Mo/Glass. The calculations of the recombination losses have been carried out based on the physical parameters of the absorber layer (thickness, absorption coefficient, mobility, etc.) and the junction (width, barrier height, carrier lifetime, etc.).

2Quantum efficiency and recombination losses

Lavagna et al [9] solved the continuity equation using the boundary conditions and they obtained an expression of the

---

* Corresponding author E-mail: hussein_abdelhafez2000@yahoo.com

quantum efficiency. This expression was simplified by Kosyachenko et al [10] and they obtained the following expression of the internal quantum efficiency.

$$\eta_{int} = \frac{1+(S_f/D_p)[\alpha+(2/W)(\varphi_o-qV)/kT]^{-1}}{1+(S_f/D_p)[(2/W)(\varphi_o-qV)/kT]^{-1}} - \frac{\exp(-\alpha W)}{1+\alpha L_n} \quad (1)$$

where, S_f denotes the recombination velocity at the front surface of the absorber, D_p is the diffusion coefficient of the holes related to the mobility μ_p by the Einstein relation $qD_p/kT= \mu_p$, α is the absorption coefficient of the absorber, W is the space-charge region width, V is the voltage, φ_o is the barrier height, L_n $(=(\tau_n D_n)^{1/2})$ is diffusion length of minority carriers, τ_n is the lifetime of electron and D_n is the diffusion coefficient of the electrons related to the mobility μ_n by the Einstein relation $qD_n/kT= \mu_n$. It should be noted that Eq. (1) does not take into consideration the recombination at the back surface of the absorber layer.

We can obtain the following expression of the known Gartner formula [11] by but $S_f=0$ in Eq.1 (in the absence of recombination):

$$\eta_{int} = 1 - \frac{\exp(-\alpha W)}{1+\alpha L_n} \quad (2)$$

Using Eq. (1) we can find an expression for the drift component of the photoelectric quantum yield. The photoelectric quantum yield that takes place in the space-charge region is equal to the absorptivity of this layer, that is, $1 - \exp(-\alpha W)$. Thus, subtracting the term $1 - \exp(-\alpha W)$ from the right side of Eq. (1), we obtain the expression for the diffusion component of the photoelectric quantum yield:

$$\eta_{diff} = \exp(-\alpha W)\frac{\alpha L_n}{1+\alpha L_n} \quad (3)$$

This equation ignores the recombination at bak survace of the absorber layer.

Subtracting the right side from Eq. 3 from the right side of Eq. 1 we come to the expression for the drift component of the photoelectric quantum yield taking into account surface recombination at the front interface:

$$\eta_{drift} = \frac{1+(S_f/D_p)[\alpha+(2/W)(\varphi_o-qV)/kT]^{-1}}{1+(S_f/D_p)[(2/W)(\varphi_o-qV)/kT]^{-1}} - \exp(-\alpha W) \quad (4)$$

The diffusion component of the internal quantum efficiency (η_{dif}) is also given from the solution of the continuity equation. The solution of the continuity equation was simplified with sufficient accuracy and can be written in the form [8],

$$\eta_{dif} = \frac{\alpha L_n}{\alpha^2 L_n^2-1}\exp(-\alpha W) \times \left\{\alpha L_n - \frac{\left(\frac{S_b L_n}{D_n}\right)[\cosh((d-W)/L_n)-\exp(-\alpha(d-W))]+\sinh((d-W)/L_n)+\alpha L_n \exp(-\alpha(d-W))}{\left(\frac{S_b L_n}{D_n}\right)sinh[(d-W)/L_n]+cosh[(d-W)/L_n]}\right\} \quad (5)$$

where S_b is the recombination velocity at back surface of the absorber layer and d its thickness.

The summation of Eq.4 and Eq.5 gives the total internal quantum efficiency with recombination losses at front and back surface of the absorber layer:

$$\eta_{int} = \eta_{drift} + \eta_{dif} \quad (6)$$

The variation of spectral internal quantum efficiency with the width of space-charge region is shown in Fig.1-a. The results of this figure are carried out at d_{CIGS}=1 µm, $S_f=10^6$ cm/s, $S_b=10^7$ cm/s and τ_n=10 ns. It can be seen that η_{int} increases with widening of the space-charge region (W) and reaches its maximum value at W=0.3 µm. This is because, more and more of the incident photons are absorbed in the space-charge region with an increase of W, where the photogenerated electrons and holes are effectively separated by the electric field. With further increase in W, the electric field in the space-charge region is reduced and recombination intensifies and then a slight decrease in η_{int} can be observed.

Quantitative characterization of the recombination losses and its effect on the solar cell performance can be obtained by calculating the short-circuit current density J_{sc}. The spectral distribution of the photons can be found as $\Phi_i / h\nu$, where Φ_i is the spectral power density, and $h\nu$ is the photon energy. The short-circuit current density (J_{SC}) can be calculated according to this formula [12]:

$$J_{SC} = q\sum_i \frac{\Phi_i(\lambda_i)}{h\nu_i}\eta_{int}(\lambda_i)\Delta\lambda_i \quad (7)$$

where Δλ is the interval between neighboring values of the wavelength.

We can determine the front surface recombination losses using Eqs.7 at $s_b=0$ (ignoring the losses at back surface) and using the flowing expression

$$Losses\ (\%) = \left(1 - \frac{Jsc}{J_{sc}^{max}}\right) \times 100 \quad (8)$$

where J_{sc}^{max} is the maximum value of short-circuit current density, which can be obtained at $S_f=0$ and $S_b=0$.

The dependence of short-circuit current density (J_{SC}) and the recombination losses on the width of space-charge region is shown in Fig.1-b. It can be noted that the maximum J_{SC} of 36.57 mA/cm^2 is achieved at W=0.3 µm. Besides the recombination losses in general are small where its maximum value is 8% which are observed at wide width of the space-charge region. In this case, the electric field does not strong enough to separate the generated carries.

According to the standard diode equation, the J(V) characteristic of a single-junction solar cell under illumination can be written as the linear superposition of the dark characteristics of the cell and the photogenerated current:

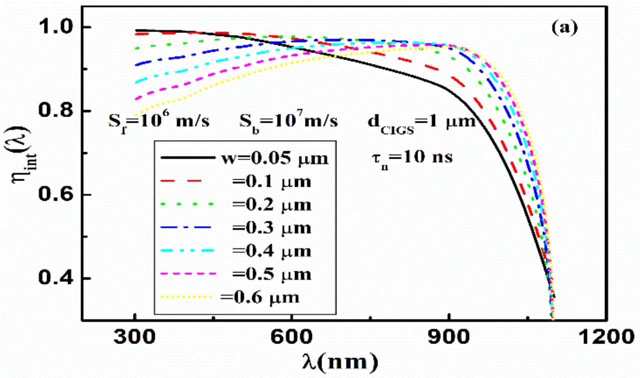

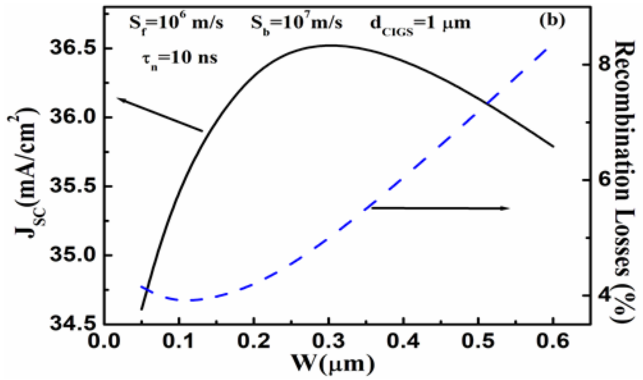

Fig.1: Variation of spectral internal quantum efficiency with the width of space-charge region (a) and the dependence of the corresponding short-circuit current density (J_{SC}) and the recombination losses on the width of space-charge region (b).

$$J = J_0\left[exp\left(\frac{qv}{AkT}\right)-1\right]-J_L \tag{9}$$

where J_L is the photogenerated current, J_0 is the reverse saturation current, q is the elementary charge, k the Boltzmann constant, T the absolute temperature and A the ideality factor. The values of J_o and A are taken from [13]. The current voltage characteristics curve (J-V) of CIGS solar heterojunction under illumination at different widths of space-charge region is shown in Fig.(2-a). The values of J_L=J_{SC} that used in these calculation have been computed based on the recombination losses as shown in Fig.1. It can be seen that there is a shift in the curves downward with widening of W until W=0.3 μm and a small shift upward can be observed with further increase in W. One of the parameters that can be estimated from this figure is the cell efficiency which can be expressed by:

$$\eta = \frac{FF\times J_{SC}\times V_0}{P_{in}} \tag{10}$$

where FF is the fill factor, V_0 is the open circuit voltage, P_{in} is the density of the total AM 1.5 solar radiation power.

Figure.2-b shows the dependence of CIGS efficiency on the width of space-charge region. It can be noted that the maximum efficiency of 25.22% is achieved at W=0.3μm under the influence of recombination losses at front and back surfaces of CIGS layer.

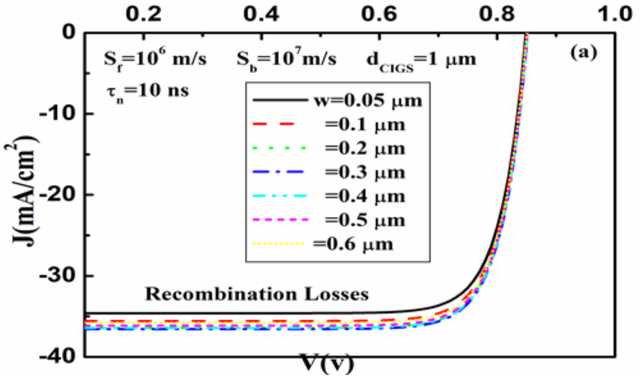

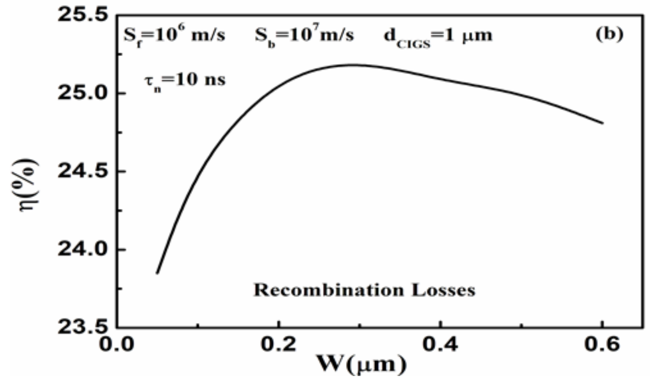

Fig.2: Current-voltage curve under illumination (a) and the efficiency (b) of CIGS solar cell as a function of the width of space-charge region considering the recombination losses.

As seen from Eq.5, the diffusion component of the internal quantum efficiency depends on the thickness of the absorber. Figure 3 represents the dependence of spectral internal efficiency and the corresponding short-circuit current density on the thickness of CIGS layer.

One can see from Fig.3-a that η_{int} increases with increasing the thickness of the absorber. A thickness of 2 μm is enough to absorb the almost total charge collection in the neutral part since no more increase in η_{int} can be observed. Such this result must be taken into consideration in fabrication this device. The dependence of J_{SC} on d_{CIGS} which plotted in Fig.3-b confirms the above result. It can be seen an abrupt increase in J_{SC} at low thickness of CIGS and it begins to saturate with further increase in d_{CIGS}. Besides, the recombination losses behave a reverse behaviour of that of J_{SC} with d_{CIGS}. Comparing the effect of W and d_{CIGS} on J_{SC} values, we concluded that the thickness of the absorber has as significant effect more than the effect of the width of the space-charge region. Accordingly, the recombination losses in later case are approximately small and are around 3% for d_{CIGS}>2 μm.

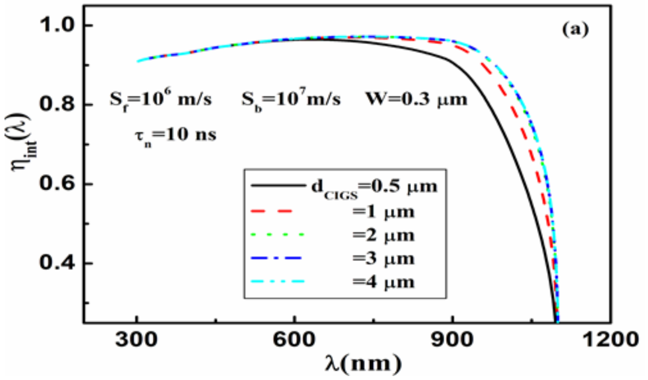

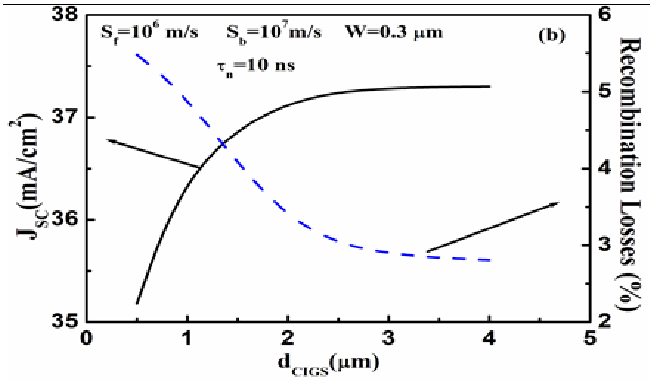

Fig.3: Dependence of spectral internal quantum efficiency on the thickness of CIGS (a) and the corresponding short-circuit current density (J_{SC}) and the recombination losses (b).

The *J*-*V* curve of CIGS solar heterojunction under illumination at different thicknesses of CIGS is shown in Fig.4-a. It can be seen that with increasing d_{CIGS} more downward shift in curves can be observed and with further increase in d_{CIGS} a saturation case happens. A maximum efficiency of about 25.8 % can be achieved at d_{CIGS} =2:3 µm as shown in Fig.4-b.

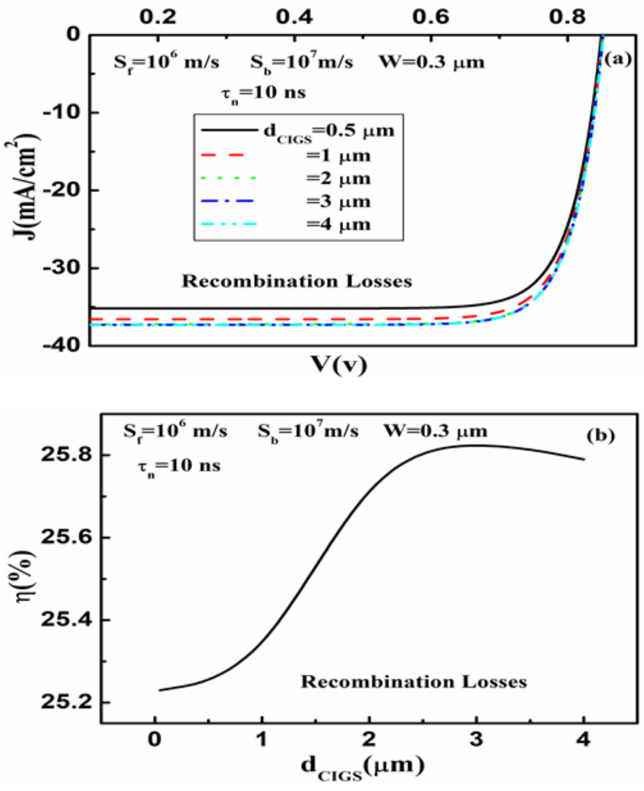

Fig.4: Current-voltage curve under illumination (a) and the efficiency (b) of CIGS solar cell as a function of the thickness of the absorber layer considering the recombination losses.

3 Front surface recombination losses

In above section, we estimated the recombination losses at front and back surface of CIGS layer. However, it is important to estimate each loss (front and back) separately. As can be seen from Eq.4 which includes the recombination losses at front surface of CIGS, the drift current and hence the front surface recombination losses depend on the recombination velocity (S_f), the width of space-charge region and on the electron lifetime. In this analysis we will study the effect of W on these losses at various values of Sf. We can determine the front surface recombination losses using Eqs.4-8 at s_b=0 (ignoring the losses at back surface). The absorption coefficient of CIGS layer is taken from ref. [6].

The dependence of short-circuit current density Jsc on the width of space-charge region W for different recombination velocity S_f in the range 10^4–10^7 cm/s (as well as S_f=0) is shown in Fig.5-a. It can be seen from this figure, if the width of space-charge region does not exceed 0.15 µm, front surface recombination does not reveal itself, but at widening of W, the decrease in Jsc becomes appreciable. The effect of the front recombination losses at S_f= 10^4 and 10^5 cm/s is very weak and can be neglected particularly at small width. At W=0.2 µm, the front surface recombination reduces the short circuit current from 37.97 to 36.49 mA/cm2 at recombination velocity of 10^4 and 10^7 cm/s, respectively. In this aspect, the front surface recombination losses are about 3.8% as shown in Fig5-b.

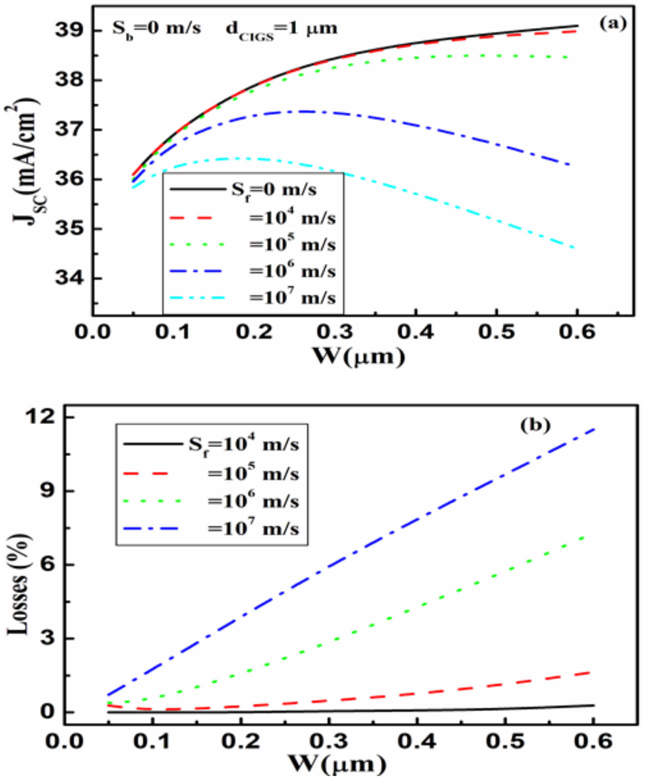

Fig.5: Short-circuit current density (a) and the corresponding front surface recombination losses (b) as a

function of the width of the space-charge region for different values of recombination velocity at the front surface of the CIGS absorber.

This small value of front surface recombination losses is due to the strong electric field in the space-charge region. As widening the space-charge region, the electric field becomes weaker and the front surface recombination losses become stronger and can record a value of about 11.5% at W=0.6 μm at high velocities of surface recombination.

4 Back surface recombination losses

As seen from Eq.5, the diffusion component of the short-circuit current depends mainly on the thickness of the absorber. If this thickness is large, the effect of recombination is imperceptible, but when the rear surface is close to the space-charge region by a distance comparable to the diffusion length of electrons, the role of recombination increases, which leads to a decrease in the diffusion component of the short circuit current. Figure 6 represents the dependences of the short-circuit current density on thickness of the absorber layer calculated for different electron lifetimes. The solid lines represent the role of back surface recombination losses ($S_b=10^6$ cm/s) while the dashed lines represent the case of neglecting these losses (at $S_b=0$).

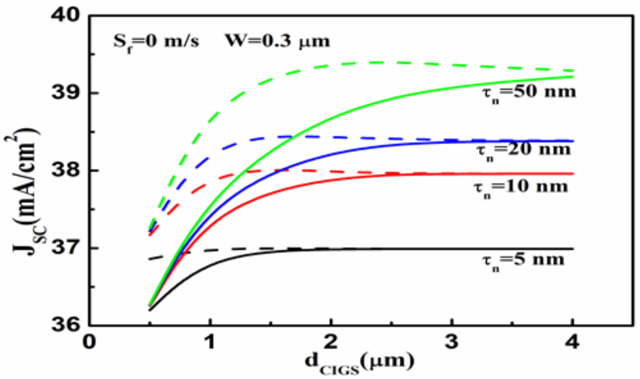

Fig.6: Dependences of the short-circuit current density on thickness of the CIGS layer calculated for different electron lifetimes with (solid lines) and without (dashed lines) taking into account recombination at the back surface of the absorber.

Note that the results of this figure are carried out at W=0.3 μm and S_f=0. As expected, the effect of recombination losses at back surface can be observed at small thickness of CIGS (<1.5 μm) and this effect can be observed at high thickness for longer minority-carrier lifetime [6]. It can be seen that at d_{CIGS}=1 μm, the recombination losses at back surface are about 0.5% for τ_n=5 ns. Besides, as the thickness of the absorber of 2 μm, the back surface recombination losses are about 0.3 % and 0.6 % at τ_n=10 ns and τ_n=20 ns, respectively. These results show that the recombination losses at back surface of CIGS layer are very small and can be neglected. It seems that with such low losses, the creation of a heavily doped layer adjacent to the back contact as it is proposed in CdS/CdTe solar cells [14] or to form a bandgap gradient outside the SCR of the CIGS absorber [15] to reduce the negative impact of recombination at the rear surface of the absorber seems apparently unreasonable.

Conclusion

In the present work, the effect of recombination losses on the performance of CIGS solar cell with structure ZnO:Al/CdS/CIGS/Mo/Glass have been studied. The calculations of the recombination losses have been carried out based on the thickness of the absorbing material, the width of space-charge region and on other parameters of the absorber layer. It can be concluded that the minimum recombination losses ate both front and back surface of the absorber layer is about 4% at 0.1 μm of the width of space-charge region. When the thickness of the absorber layer reaches 4 μm, the recombination losses record a minimum value of about 2.7 %. The back surface recombination losses are so small and then can be neglected. The thin-film CIGS solar cell efficiency records high efficiency of 25%.

References

[1] Carron R., Nishiwaki S., Feurer T., et al., Advanced Energy Materials., **9**, 1900408 (2019),.

[2] Zhang X., Kobayashi M., Yamada A., ACS Appl. Mater. Interfaces., **9**, 16215(2017).

[3] Delahoy, A. E., Chen, L., Akhtar, M., Sang, B., Guo, S., Sol. Energy., 77, 785 (2004).

[4] Nakamura M., Yamaguchi K., Kimoto Y., et al., Journal of Photovoltaics., **9**, (18632019).

[5] http://www.nrel.gov/ncpv/images/efficiency_chart.jpg

[6] Kosyachenko, L. A., Mathew, X., Paulson, P. D., Ya. Lytvynenko, Maslyanchuk, V. O. L., Solar Energy Materials & Solar Cells., **130**., 291–302 (2014).

[7] Khoshsirata, N., Yunus, N.A.M., Hamidon, M.N., Shafie S., Amin, N., Optik., 126, 6 81(2015).

[8] Belghachi, A., Limam, N., Chinese Journal of Physics ., **55**, 1127–1134(2017),

[9] Lavagna, M., Pique, J.P., Marfaing, Y. *Solid State Electronics.*, **20**, 235-240(1977).

[10] Kosyachenko, L.A., Sklyarchuk, V. M., Sklyarchuk, Ye.F., Ulyanitsky, K.S., *Semicond. Sci. Technol.*, **14**, 373-377(1999).

[11] Gartner W.W., *Phys. Rev.*, **116**, 84-87(1959).

[12] Mohamed, H. A., Mohamed A. S. and Ali, H. M. Mater. Res. Express., **5**, 056411(2018).

[13] Wang, W., Winkler, M. T., Gunawan, O. T., Todorov, T. K., Zhu, Y., Mitzi, D. B., Adv. Energy Mater., **4**, 1301465(2014).

[14] Kosyachenko, L. A. Mathew, X., RoshkoV. Ya., Grushko,E. V., Sol. Eng. Mater. Sol. Cells., **114**, 179–185(2013).

[15] Shafarman, W. N., Siebentritt, S. Stolt, L., Handbook of Photovoltaic Science and Engineering, 2nd ed., John Wiley & Sons, Ltd., West Sussex, UK., 546–599(2011).